The International Journal of Advanced Manufacturing Technology
https://doi.org/10.1007/s00170-017-1452-1

ORIGINAL ARTICLE

Sustainability analyses of cutting edge radius on specific cutting energy and surface finish in side milling processes

Isuamfon F. Edem [1] · Vincent A. Balogun [2]

Received: 30 September 2017 / Accepted: 28 November 2017

Abstract

The aim of this work is to determine the influence of cutting edge radius on the specific cutting energy and surface finish in a mechanical machining process. This was achieved by assessing the direct electrical energy demand during side milling of aluminium AW6082-T6 alloy and AISI 1018 steel in a dry cutting environment using three different cutting tool inserts. The specific energy coefficient was evaluated as an index of the sustainable milling process. The surface finish of the machined parts was also investigated after machining. It was observed that machining with the 48.50-μm cutting edge radius insert resulted in lower specific cutting energy requirements when compared with the 68.50 and 98.72-μm cutting edge radii inserts, respectively. However, as the ratio of the undeformed chip thickness to cutting edge radius is less than 1, the surface roughness increases. The surface roughness values gradually decrease as the ratio of undeformed chip thickness to cutting edge radius (h/r_e) tends to be 1 and at minimum surface roughness values when the ratio of h/r_e equalled to 1. However, the surface roughness values increased as h/r_e becomes higher than 1. This machining strategy further elucidates the black box and trade-offs of ploughing and rubbing characteristics of micro machining and optimization strategy for minimum energy and sustainable manufacture.

Keywords Sustainability · Specific cutting energy · Mechanical machining · Nose radius · Cutting edge radius · Surface roughness

Nomenclature

h	Undeformed chip thickness in millimetres
r_e	Cutting edge radius in millimetres
E_{spec}	Specific energy
P_0	Constant or baseline power demand of the machine tool in W
Q	Material removal rate (MRR) in cubic millimetres per second
k	Specific cutting energy of the material in joules per cubic millimetre
a_p	Depth of cut in millimetres*mm.*
a_e	Width of cut in millimetres
f	Feed rate in millimetres per revolution
h_{avg}	Average undeformed chip thickness in millimetres
V_c	Cutting speed in metres per minute
f_z	Feed per tooth in millimetres per tooth
P	Total power drawn by the machine tool in W
φ	Swept angle in degree
φ_s	Swept angle in radian
φ_1	and φ_2 Swept angles which are equal to zero either at entrance of the tool into the workpiece or at exit of the tool
R_a	Surface roughness in micrometres

Electronic supplementary material The online version of this article (https://doi.org/10.1007/s00170-017-1452-1) contains supplementary material, which is available to authorized users.

✉ Isuamfon F. Edem
isuamfon@gmail.com

[1] Faculty of Engineering, Department of Mechanical Engineering, Akwa Ibom State University, Ikot Akpaden, Mkpat Enin, Akwa Ibom State, Nigeria

[2] Faculty of Engineering, Department of Mechanical Engineering, Edo University Iyamho, Iyamho, Edo State, Nigeria

1 Introduction

In the electrical energy breakdown analysis, machine tools consume about three quarters of the total electrical energy required for the machining process and one quarter for the actual material removal process [1, 2]. The consumed electrical energy of the machine tool could be classified as the basic [3, 4], the ready [5, 6], and the cutting energy states [7]. Recommendations were made by ISO 14955-1 [8] and the cooperative effort on process emissions in manufacturing (CO2PE!) [9] for sustainable machining and for the development of green machine tools. In addition, the European Union (EU) member states agreed on the principle of 20/20/20 by the year 2020 in order to achieve a 20% reduction in greenhouse

Published online: 11 December 2017

gases, a 20% share of renewable energies, and a 20% increase in energy efficiency as compared to the 1990 indicators [10].

Guo et al. [11] stated that the specific energy could be used to determine the amount of energy consumed based on the surface roughness of the machined surface. The specific energy is the energy required by the machine tool to remove a unit volume of a material from a workpiece as proposed by Gutowski et al. [3] and stated in Eq. 1.

$$E_{spec} = \frac{P_0}{Q} + k \tag{1}$$

where P_0 is the constant power demand of the machine tool and Q represents the material removal rate (MRR) in cubic millimetres per second; k is the specific cutting energy of the material in joules per cubic millimetre.

1.1 Specific energy, machining efficiency, and size effect

It has been reported that the specific energy could be a measure of the efficiency of the machining process [12, 13]. Based on these inferences, it can be deduced that machining efficiency allows products and processes to be assessed based on scientific values related to power demand and material removal rates (MRR) such as depth of cut, feed rate, and the width of cut [13]. Specific cutting energy could be significantly influenced by different factors. These could include the type of machining (continuous or intermittent, dry or wet), cutting parameters (depth of cut, width of cut, cutting speed, feed rate), workpiece properties (hardness), cutting tool (tool geometry, tool material), and the undeformed chip thickness [14, 15].

It is well documented that the ratio of undeformed chip thickness to cutting edge radius significantly influences chip formation in milling operations. This is apart from the tool geometry and workpiece material characteristics being some of the factors affecting the determination of minimum chip thickness for chip formation. Thus, the minimum chip thickness is the ratio of feed per tooth to the cutting edge radius below which no chips are formed, and is referred to as the lower limit of machining. Yuan et al. [16] proposed the theoretical minimum cutting edge ratio to be 0.2–0.4 when cutting steel with carbide or high-speed steel tools. They argued that the proposed ratio depends on the friction between tool-chip interface. Machining below this value resulted in high-friction forces induced by plastic deformation and intense rubbing. Bissacco et al. [17] stated that if the ratio of undeformed chip thickness (feed per tooth) to cutting edge radius is less than 1, then the process is dominated by intense rubbing and ploughing which defines the size-effect phenomenon in micro machining. The size effect phenomenon increases the specific cutting forces in the cutting process [18] and enhances a nonlinear increase in specific cutting force, which has been the basis for empirical force modelling in machining [19]. Thus, the specific cutting energy could be influenced by the size effect, cutting mechanisms, and the chip thickness.

Few researchers have undertaken studies on specific energy demand and cutting parameters in machining. Sarwar et al. [13] maintained that useful information on the machinability of workpiece materials could be obtained from the variation of specific energy. Guo et al. [11] showed that the specific cutting energy increased with cutting speed, and decreased with increase in both depth of cut and width of cut. Balogun and Mativenga [20] showed that feed rates can significantly influence the specific cutting energy of materials and that a minimum specific energy ensued when machining at feed rates higher than the cutting edge radius for aluminium AW6082-T6 alloy, AISI 1045 steel alloy, and titanium 6Al-4V alloy. However, this work only investigated the cutting tool insert with 0.4-mm nose radius. Also, the influence of cutting edge on the surface roughness was not considered. Balogun et al. [21] studied the impacts of chip thickness, tool wear, nose radius, and cutting environment on the specific cutting energy in mechanical machining processes. It was reported that the specific energy decreases from 5.34 to 1.47 J/mm^3 when machining AISI 1045 steel at feeds between 0.01 and 0.55 mm/tooth, respectively. This means that specific energy was minimised by 72% resulting in 18% reduction in the total direct energy demand. It was also shown that an increase in the undeformed chip thickness up to the point where it is higher than the cutting edge radius results in minimal specific energy demand. However, this work did not capture the impact of undeformed chip thickness on the surface roughness of the machined parts considering different nose radii. Schluter et al. [22] used experimental design techniques, regression models, and Taguchi loss function to optimise cutting parameters for minimum specific cutting energy and improved surface finish. The authors reported that lower specific cutting energy and surface roughness were obtained when the depth of cut a_p was set at 2.34 mm, width of cut a_e at 33.4 mm, and feed rate f at 0.44 mm/rev. Nevertheless, the effect of cutting edge radius on specific energy efficiency and surface roughness was not considered in this study.

Sealy et al. [23] also reported that tool wear had the dominant influence on increasing the specific cutting energy when compared with feed rate and depth of cut, while Liu et al. [24] reported that the influence of tool wear on the total specific energy demand was significant at the process level, and minimal at both the machine tool and spindle levels. Balogun et al. [25] performed side milling tests on a 3-axis CNC milling machine in order to investigate the specific ploughing energy on aluminium AW6082-T6 alloy, AISI 1045 steel alloy, and titanium 6Al-4V alloy materials. This was achieved by studying the correlation between the specific ploughing energy and

cutter swept angle to identify an optimum undeformed chip thickness and width of cut for minimal ploughing effects. The authors showed that minimum specific ploughing energy occurred at an optimal swept angle of 39.74° when machining with a tool having a cutting edge radius of 60 μm. Although three different workpiece materials were considered in this study, only 0.4-mm nose radius cutting tool insert was considered. Wang et al. [26] studied the specific cutting energy required to produce serrated chips of 7050-T7451 aluminium alloy in high-speed milling. From their results, it was found that minimal specific cutting energy was obtained when machining with cutting tools which possessed large positive rake angles. Zhou et al. [27] developed a specific energy consumption (SEC) model for predicting the cutting power on a milling machine. Their study was based only on the relationship between spindle rotation speed, cutting parameters, material removal rate, specific energy consumption, cutting power, and material removal power.

Machining with large undeformed chip thickness is also recommended for improved surface roughness. Recently, Balogun and Edem [28] investigated the influence of swept angle optimisation on the specific cutting energy in milling AISI 1045 steel alloy. It was reported that lower specific cutting energy and ploughing effects could be obtained at an optimum swept angle value of 31.8°, while a swept angle value of 41.4° increased the specific cutting energy and machine tool power. This paper, however, did not consider the influence of cutting tool nose radius on the specific cutting energy and surface finish in line with the step over variations for the optimization criterion.

1.2 Specific cutting energy and cutting edge radius

Experimental studies to determine the effects of cutting edge radius on the specific cutting energy in mechanical machining have been well documented in literature. For example, Taminiau and Dautzenberg [29] performed cutting tests on a brass workpiece with low undeformed chip thickness values (feed rates varying between 0.04 and 0.2 mm), resulting in high cutting energy. The authors, having used to macro tool inserts with cutting edge radii ranging between 50 and 200 μm, as well as diamond tool with edge radius of 15 μm, found that cutting forces increased based on the ratio between the undeformed chip thickness and cutting edge radius. Waldorf [30] undertook experimental analysis with varying chamfer and edge-hone geometry of cutting tool inserts to conduct turning tests. The authors reported that cutting forces were significantly influenced by the varying cutting tool geometries. Additionally, high cutting forces were observed with increase in cutting edge radius. However, inserts with different nose radii were not considered in the study. Arif et al. [31] performed cutting tests on tungsten carbide plates with thickness of 0.5 mm using a 3-axis vertical spindle machine. It was found that increase in cutting edge radius resulted in high-specific cutting energy and an improved material removal rate due to increased cutting edge radius of 5.92 μm. Zhang et al. [32] investigated the influence of size effect on the specific cutting energy in micro-orthogonal cutting of AISI 1045 steel. This was achieved by utilising the slip-field model to analyse the deformation process of workpiece material. It was observed that specific cutting energy is greatly influenced by size effect due to shear strain hardening, shear strain rate hardening, shear temperature softening, and relative cutting length as a result of the ratio of undeformed chip thickness to cutting edge ratio. Nevertheless, influence of tool cutting tool edge radius on surface roughness of the machined part was not considered.

1.3 Surface roughness and cutting edge radius

Few researchers also studied the influence of cutting tool edge radius on surface finish of machined parts. In one of their studies based on micromachining strategies, Vogler et al. [33] determined the surface roughness of workpiece on which inserts with different cutting edge radii were used. They discovered that using an insert with 5-mm cutting edge radius increased the surface roughness when compared with an insert with 2-mm cutting edge radius. This phenomenon was also confirmed by Chou and Song [34] during the study of the effect of tool nose radius on surface roughness and tool wear performing finish hard turning of AISI 52100. A lower ratio of the undeformed chip thickness and the cutting edge radius also influence surface finish of machined components [35]. This ratio may increase the ploughing effects and cutting forces during the machining process. Zhao et al. [36] undertook an experimental study to investigate the effect of cutting edge radius on surface roughness and tool wear in hard turning of AISI 52100 steel using CBN cutting tools with nominal edge radii of 20, 30, and 40 μm. It was observed that the cutting tool with nominal cutting edge radius of 30 μm resulted in lower surface roughness and lower tool wear. Nonetheless, this study did not investigate the influence of cutting edge radius on specific cutting energy. Fulemova and Janda [37] studied the influence of cutting edge preparation and cutting edge radius on surface roughness of the machined part, tool life, and cutting forces when machining ferrite-martensite stainless steel with carbide inserts. It was reported that the cutting tool with 15-μm cutting edge radius resulted in higher tool life, lowest roughness, and lowest force load when compared with the tools with 5- and 10-μm cutting edge radii, respectively.

From reviewed literature, insights into the effects of the ratio of the undeformed chip thickness to the cutting edge radius, as well as the cutting edge radius on the specific cutting energy has been presented by few researchers. However, the effect of cutting tool edge geometry on the specific cutting

energy and surface finish when milling two workpiece materials is relatively unexplored. This gap would be investigated in this study. This would provide recommendations for improving energy efficiency, surface finish, and mechanical machining sustainability in order to determine ways to reduce associated environmental impacts. Also, it would provide valuable data and knowledge for resource efficient machining through reduction in electrical energy demand and improved surface finish.

1.4 Research aim

This work aims at determining the trade-offs and influence of cutting edge radius on the specific cutting energy and surface finish in a mechanical machining process. This was achieved by assessing the direct electrical energy demand for side milling of aluminium AW6082-T6 alloy and AISI 1018 steel in a dry cutting environment using three similar inserts with different nose and cutting edge radii, while the electric current drawn was measured. Further studies were conducted by checking the surface finish of the side-milled parts with different cutting tool edge radii.

2 Experimental details

2.1 Experimental setup

In order to determine the influence of different insert noses and cutting edge radii on the specific cutting energy, side milling of aluminium AW6082-T6 alloy and AISI 1018 steel was performed in a dry cutting environment with three (3) square single insert types. The cutting tool inserts employed were SOMT-060204-HQ IC328, SOMT-060208TN-HQ IC328, and SOMT 060216TN-HQ IC328 with nose radii of 0.4, 0.8, and 1.6 mm as shown in Fig. 1a–c, respectively.

The side milling tests were conducted on the Mikron HSM 400 milling machining centre with a Heidenhain TNC 410 NC controller for display and insertion of NC codes. This machine tool has a HVC 140-5B-10-15/42-3F-HSK-E40 spindle manufactured by STEP-TEC with a speed as high as 42,000 rev/min and feed rates up to 40,000 mm/min for each of the x, y, and z-axes, respectively. The machine tool construction has the table moving along the x-axis direction (horizontal), the spindle moving along the y-axis direction (transverse), and the spindle descending or retracting along the z-axis direction (vertical). The mass of the x-axis modelled from solid works software was approximately 430 kg, while the mass of the y- and z-axes was approximately 250 kg [38]. The x, y, and z-axes accelerate at 10 ms^{-2} with rated power requirements of 11 kW for the x-axis and 14.8 kW for the y- and z-axes. The spindle motor has a rated power of 13 kW. The axes' drives are powered by the AC servo motors with direct linear drive mechanisms. Figure 2 shows the workpiece and cutting tool setup on the machine tool for the cutting test.

2.2 Experimental procedures

Flat bars of aluminium AW6082-T6 alloy and AISI 1018 steel with dimensions of 100 × 40 ×3.5 mm were received from the manufacturers. The workpiece materials were rigidly mounted on the machine tool vice with a maximum overhang of 15 mm in order to reduce the vibrations from the workpiece material and cutting tool. The inserts were mounted on an 8-mm diameter single flute tool holder Iscar EX90-D08-C10-06 with an overhang of 25 mm as in Fig. 2. The cutting parameters were adapted from the insert manufacturers' process window. Details of the workpiece and cutting parameters are presented in Tables 1 and 2.

The feeds (chip loads) and radial widths of cut were varied from 0.01 to 0.37 mm/tooth and from 0.25 to 1.0 mm for both materials, respectively. The depth of cut was determined by the workpiece thickness and kept constant at 3 mm. Different material removal rates were obtained by varying the radial width of cut. The side milling process was performed by utilising only the straight cutting edge of the insert in order

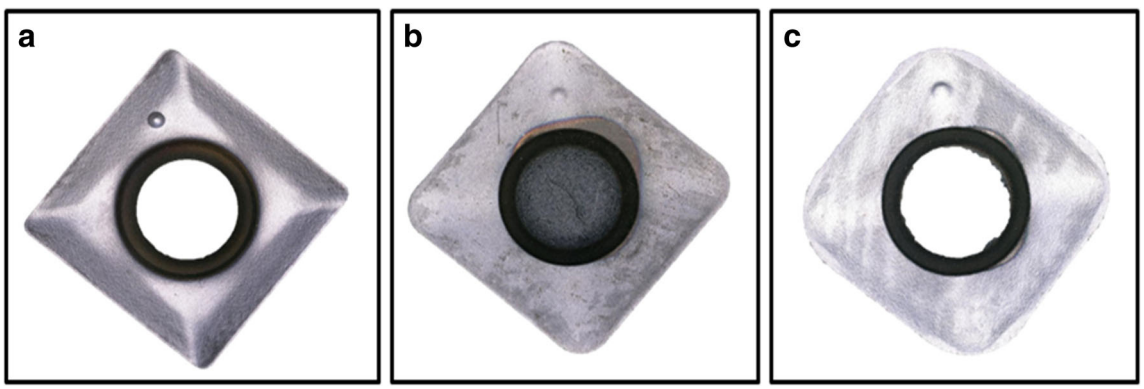

Fig. 1 **a** Iscar SOMT-060204-HQ IC328. **b** Iscar SOMT-060208TN-HQ IC328. **c** Iscar SOMT 060216TN-HQ IC328

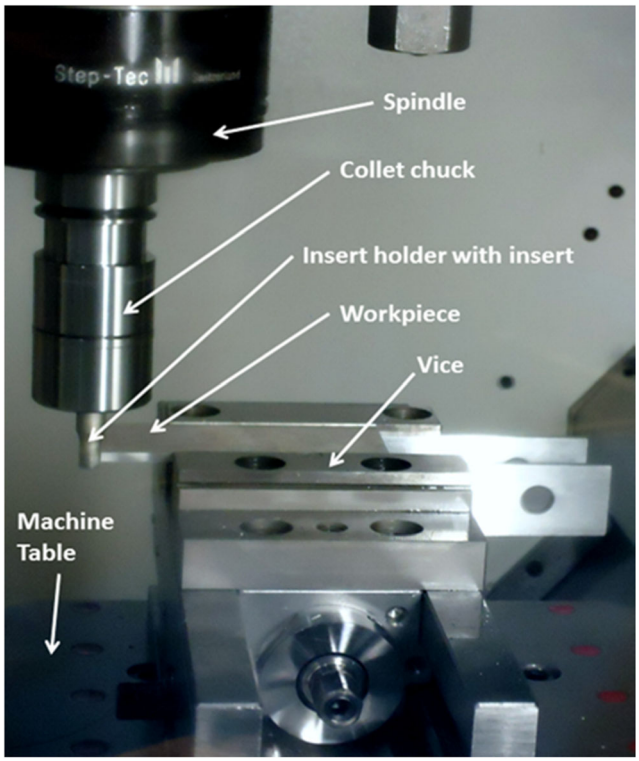

Fig. 2 Setup for side milling operation on Mikron HSM 400 milling machining centre

to prevent the nose radius of the insert from being engaged during the cutting process. Each side milling test was conducted three times for consistencies.

The cutting tool edge was observed and measured under the Keyence VHX-500 Digital microscope. This was achieved by drawing a circle of best fit with the tangential line intersecting the flank and rake faces of the insert, and the measured value was automatically evaluated by the microscope as shown in Fig. 3 and tabulated in Table 3.

A new cutting edge was employed at each feed rate for each of the cutting test repeated three times for each of the 48.50, 68.50, and 98.72 μm cutting tool edge radii, respectively. The power requirement of the CNC milling machine during the cutting tests were measured and recorded with the 3-phase Fluke 434 power quality analyser. Thus, the specific energy coefficients for the two workpiece materials were determined from the power_material removal rate (MRR) graph. Additionally, the surface roughness of the side-milled parts was evaluated using the Surtronic 25 portable surface roughness checker.

Table 1 Workpiece parameters

Workpiece material	Aluminium AW6082-T6 alloy	AISI 1018 steel (low carbon steel)
Length of workpiece, (mm)	100	100
Width of workpiece, (mm)	40	40
Workpiece thickness, (mm)	3.5	3.5
Chemical composition of workpiece	1% Mn, 0.5% Fe, 1.2% Mg, 1.3% Si, 0.1% Cu, 0.2% Zn, 0.1% Ti, 0.25%Cr, balance Al	0.17% C, 0.27% Si, 0.80% Mn, 0.050% S max, 0.050% P max
Workpiece hardness, HV	111.1, 118.3, 109.3, 106.7, 105.2, 106 Average = 109.43	191, 236, 226, 224, 236, 287 Average = 233.3
Workpiece mass, (g)	37.97	111.09

3 Results and discussions

3.1 Cutting edge radius and the specific cutting energy trade-offs

The graph of power_material removal rate (MRR) during the side milling of aluminium AW6082-T6 alloy using inserts with 48.50, 68.50, and 98.72 μm cutting edge radii at chip load of 0.01 mm/tooth are as shown in Fig. 4a–c, respectively.

Considering Fig. 4a–c, it can be observed that power demand increases with the material removal rates when machining aluminium AW6082-T6 alloy with inserts of 48.50, 68.50, and 98.72μm cutting edge radii at chip load of 0.01 mm/tooth.

Figure 5a–c presents graphs of power_MRR during side milling of AISI 1018 steel with 48.50, 68.50, and 98.72 μm cutting edge radii at chip load of 0.01 mm/tooth.

Other chip loads of 0.19, 0.28, and 0.37 mm/tooth were also considered, and their respective graphs were plotted. An increasing straight line trend of the power_MRR relationships was also observed. Thus, the specific energy coefficients (slopes) of the resulting graphs in Figs. 4 and 5 and for all the milling trials were used to derive the specific cutting energy coefficients at different feeds (chip loads) and cutting edge radii for aluminium AW6082-T6 alloy and AISI 1018 steel. These are presented in Tables 4 and 5 for aluminium AW6082-T6 alloy and AISI 1018 steel, respectively.

The specific energy coefficients deduced in Tables 4 and 5 were further correlated with feeds in order to determine the influence of feeds on the specific energy demand when performing side milling on two different workpiece materials using inserts with varying cutting edge radii and are presented in Figs. 6 and 7 for AW6082-T6 alloy and AISI 1018, respectively.

From Figs. 6 and 7, it can be observed that the specific cutting energy decreases as the feed increases from 0.01 to 0.37 mm/tooth. The specific cutting energy is higher at feeds of 0.01 mm/tooth than at feeds of 0.37 mm/tooth for AW6082-T6 alloy and AISI 1018 due to the fact that more rubbing and ploughing effects are experienced at lower feeds (i.e. 0.01–0.1 mm/tooth) than at higher feeds (i.e. 0.19–0.37 mm/tooth).

Table 2 Cutting parameters

Type of machine tool	Mikron HSM 400 milling machining centre	
Workpiece material	Aluminium AW6082-T6 alloy	AISI 1018 steel
Chip load, f_z (mm/tooth)	0.01–0.37	0.01–0.37
Radial width of cut, a_e (mm)	0.25–1.00	0.25–1.00
Cutting speed, V_c (m/min)	250	100
Spindle speed, N (rev/min)	10,000	4000
Diameter of cutting tool, D (mm)	8	8
Cutting tool holder	EX90-D08-C10–06	EX90-D08-C10–06
Cutting tool insert type	i) SOMT-060204-HQ IC328	i) SOMT-060204-HQ IC328
	ii) SOMT-060208TN-HQ IC328	ii) SOMT-060208TN-HQ IC328
	iii) SOMT-060216TN-HQ IC328	iii) SOMT-060216TN-HQ IC328
Number of teeth/flutes, z	1	1

This also confirms the work of Balogun et al. [25], that at lower feeds, the undeformed chip thickness is lower than the cutting edge radius and hence induces ploughing and rubbing mechanisms at the tool workpiece interface. At the same time, the ploughing and rubbing mechanisms increase the tool wear at the tool chip contact interface thereby increasing the curvature and the contact length of the cutting edge. This phenomenon increases the tool nose radius which makes shearing and deformation of material difficult, thereby increasing the specific cutting energy coefficient as shown in Figs. 6 and 7.

Also, cutting tools with large nose radius possess increased cutting edge which in turn reduces the undeformed chip thickness, enhances size effect, and increases the specific cutting energy [39]. Thus, the graphs in Figs. 6 and 7 show that performing side milling on the specified workpiece materials with the 48.50-μm cutting edge radius insert resulted in lower specific energy requirements when compared with the 68.50 and 98.72-μm cutting edge radii inserts. This could be due to the smaller and sharper cutting edge radius of the 0.4-mm radius insert, which in turn reduces the cutting forces and friction between the tool-chip interface.

For the purpose of evaluating the relationship between the specific cutting energy and the undeformed chip thickness h_{avg}, it is important to calculate the values of h_{avg} for all engaged chip loads. The average undeformed chip thickness h_{avg} is estimated using Eqs. 2a and 2b [25].

$$h_{avg} = \frac{f_z}{\varphi_s}\int_{\varphi_1}^{\varphi_2} \sin\varphi \mathrm{d}\varphi \tag{2a}$$

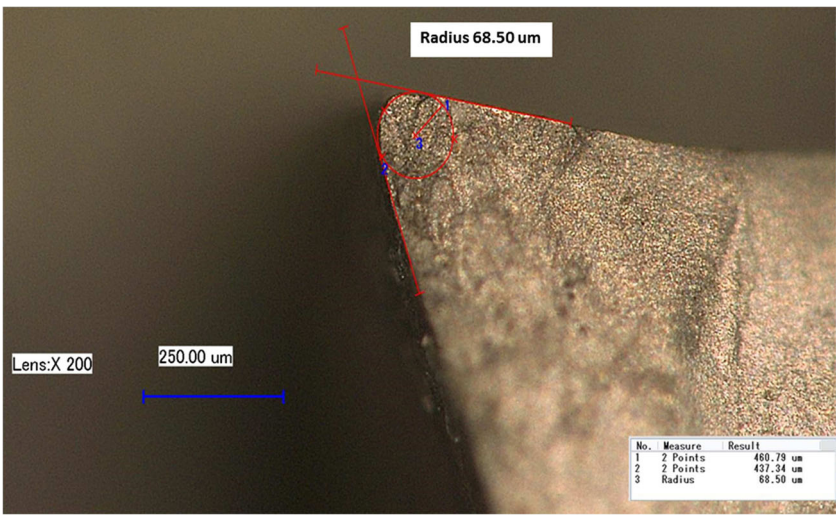

Fig. 3 Cutting edge radius measurement for insert with 0.4-mm nose radius

Table 3 Cutting tool geometry

Cutting tool insert type	SOMT-060204-HQ	SOMT-060208TN-HQ	SOMT 060216TN-HQ
Nose radius of insert (mm)	0.4	0.8	1.6
Average cutting edge radius (μm)	48.50	68.50	98.72
Rake angle (°)	5	5	5
Clearance angle (°)	7	13	13

$$h_{\mathrm{avg}} = \frac{f_z}{\varphi_s}[-\cos\varphi]_0^{\varphi} \tag{2b}$$

where h_{avg} is the average undeformed chip thickness (mm), f_z is the feed per tooth (mm/tooth), φ is the swept angle in degree and φ_s is the swept angle in radian, φ_1 and φ_2 are equal to zero either at entrance of the tool into the workpiece or at exit of the tool. The swept angle depends on the radial width of cut and the diameter of the tool.

The trend of the relationship between the specific cutting energy and undeformed chip thickness for different workpiece material and different cutting edge radii employed in the milling trials is similar to Figs. 6 and 7.

Higher values of specific cutting energy are obtained at undeformed chip thickness of 0.01 mm due to increased rubbing and ploughing effects, which is more appropriate for a finishing operation. Also, machining at this undeformed chip thickness means that highly negative rake angles are engaged during cutting. As the undeformed chip thickness tend to increase, the specific energy reduces due to transition of machining process mechanism into the dominant shearing cutting region with little effects of ploughing. Hence, mechanical machining should be encouraged at this process domain since machining tends to be more sustainable at the shearing process mechanism domain. These results could also be used to evaluate the trade-offs between cutting edge radius and energy demand. It is important to know that depending on the machining strategy (i.e. roughing or finishing) required, selection of the appropriate process parameters is paramount to sustainable machining as can be deduced from Figs. 6 and 7. Selecting lower undeformed chip thickness could lead to higher specific energy demand.

3.2 Surface finish induced by different cutting edge radii

The surface roughness (R_a) analysis was conducted when performing side milling of aluminium AW6082-T6 alloy and AISI 1018 steel at the radial width of cut of 1.00 mm. This data is important for determining the correlation between surface roughness and the ratio of undeformed chip thickness to cutting edge radius when considering inserts with different nose and cutting edge radii. The surface roughness of the milled parts was measured with Surtronic 25 portable surface roughness checker. Readings were performed three times. Figures 8 and 9 show graphs of surface roughness and the ratio of undeformed chip thickness to cutting edge radius for aluminium AW6082-T6 alloy and AISI 1018 steel, respectively, when machining with inserts of different cutting edge radii.

Figures 8 and 9 show higher surface roughness values when the ratio of the undeformed chip thickness to the cutting edge radius is lower than 1 for different workpiece materials. This means that this region is dominated by rubbing and ploughing effects. A decreasing trend of surface roughness values is noticed when the ratio of undeformed chip thickness to cutting edge radius (h/r_e) tends to be 1. Minimum surface roughness values were obtained as the ratio of h/r_e=1. However, the surface roughness values increased as the ratio of undeformed chip thickness to cutting edge radius was higher than 1. This may be due to the influence of higher feeds (chip load) which leaves feed marks on the side-milled surfaces of the two different workpiece materials.

Additionally, it is observed from Figs. 8 and 9 that side milling with the 48.50-μm cutting edge radius insert resulted in lower surface roughness values due to its lower cutting edge radius when compared with the 68.50 and 98.72-μm cutting edge radii inserts. This is because the 0.4-mm nose radius insert has a smaller cutting edge radius, which makes it sharper and therefore results in lower friction between the tool and workpiece, and lower ploughing and rubbing effects. However, machining with large cutting edge radius leaves visible feed marks on the newly machined surface. In view of this, it is recommended that inserts with smaller cutting edge radius should be employed for improved energy efficiency and surface finish in mechanical machining of parts. This could also favour sustainable manufacture of products.

4 Conclusions

This work aimed at analysing the influence of inserts with different nose and cutting edge radii on the specific cutting energy and surface finish in a mechanical machining process. The following conclusions were obtained from this study:

- The specific cutting energy decreases as the chip load increases from 0.01 to 0.37 mm/tooth due to the fact that more rubbing and ploughing effects were experienced at

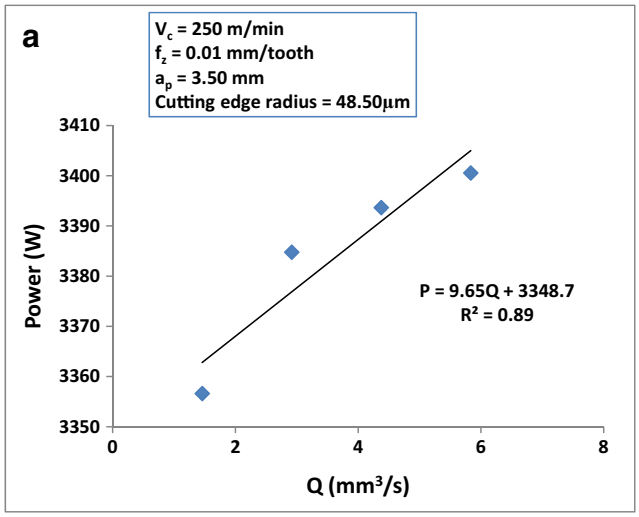

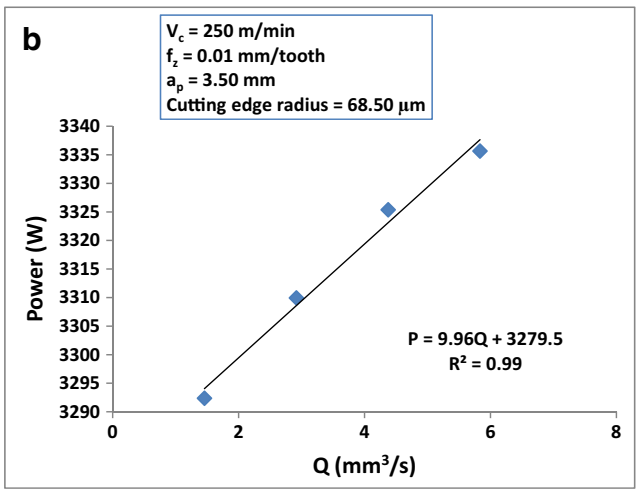

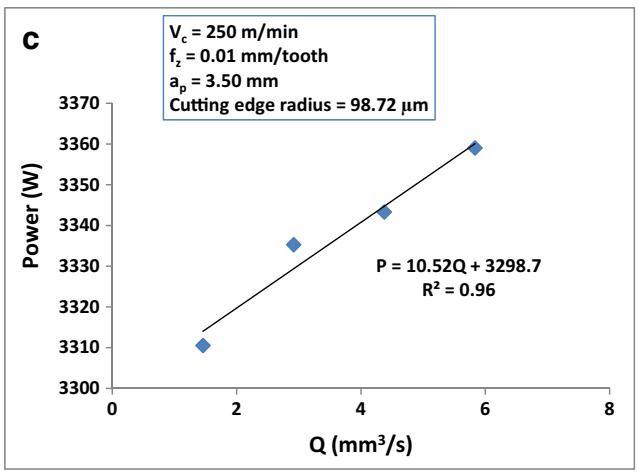

Fig. 4 **a** Power_MRR during side milling of aluminium AW6082-T6 alloy using 48.50 µm cutting edge radius insert. **b** Power_material removal rate (MRR) during side milling of aluminium AW6082-T6 alloy using 68.50 µm cutting edge radius insert. **c** Power_material removal rate (MRR) during side milling of aluminium AW6082-T6 alloy using 98.72 µm cutting edge radius insert

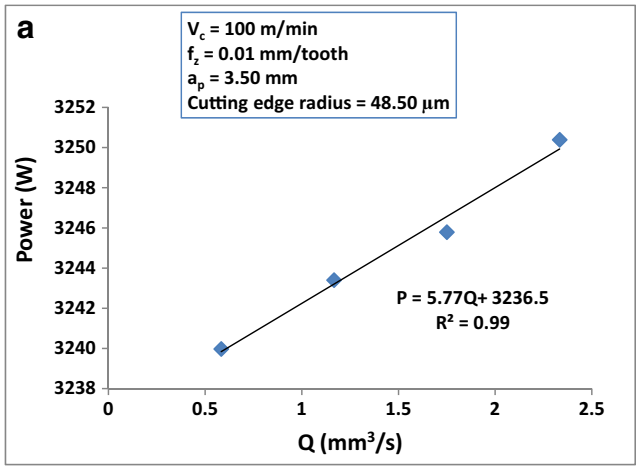

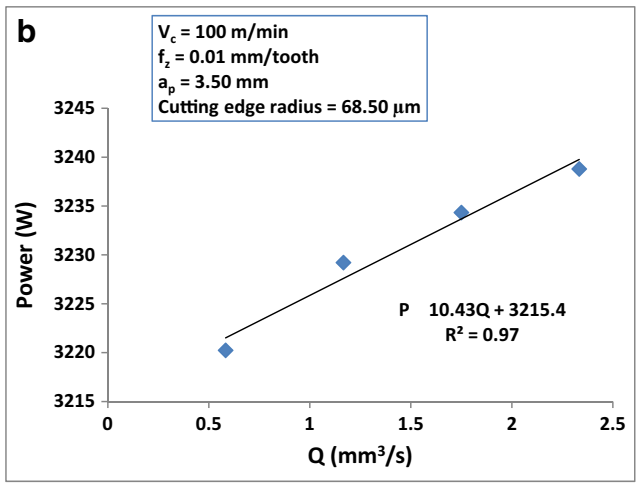

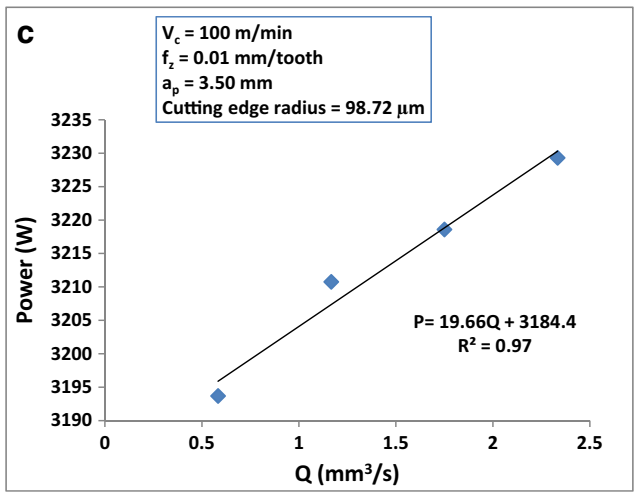

Fig. 5 **a** Power_material removal rate (MRR) during side milling of AISI 1018 steel using 48.50-µm cutting edge radius insert. **b** Power_material removal rate (MRR) during side milling of AISI 1018 steel using 68.50-µm cutting edge radius insert. **c** Power_material removal rate (MRR) during side milling of AISI 1018 steel using 98.72-µm cutting edge radius

lower feeds than at higher feeds. This study also shows that the undeformed chip thickness is lower than the cutting edge radius at lower feeds.

Table 4 Specific energy coefficients of the graphs for side milling of aluminium AW6082-T6 alloy with different cutting edge radii

Chip load (mm/tooth)	48.50-µm cutting edge radius		68.50-µm cutting edge radius		98.72-µm cutting edge radius	
	Slope (J/mm^3)	R^2	Slope (J/mm^3)	R^2	Slope (J/mm^3	R^2
0.01	9.65	0.89	9.96	0.99	10.53	0.96
0.10	1.04	0.96	1.62	0.91	1.43	0.98
0.19	0.69	0.99	0.48	0.99	0.54	0.99
0.28	0.54	0.99	0.34	0.99	0.38	0.94
0.37	0.26	0.97	0.33	0.99	0.33	0.96

Table 5 Specific energy coefficients for side milling of AISI 1018 steel with different cutting edge radii

Chip load (mm/tooth)	48.50-µm cutting edge radius		68.50-µm cutting edge radius		98.72-µm cutting edge radius	
	Slope (J/mm^3)	R^2	Slope (J/mm^3)	R^2	Slope (J/mm^3)	R^2
0.01	5.77	0.99	10.43	0.97	19.66	0.97
0.10	1.62	0.97	1.88	0.99	4.18	0.94
0.19	0.85	0.98	0.98	0.99	2.16	0.99
0.28	0.72	0.75	0.79	0.99	2.12	0.99
0.37	0.51	0.97	0.66	0.99	1.20	0.97

- Undertaking side milling on aluminium AW6082-T6 alloy and AISI 1018 steel workpiece materials with the 48.50-µm cutting edge radius insert resulted in lower specific cutting energy when compared with the 68.50 and 98.72-µm cutting edge radii inserts. This could be due to the smaller cutting edge radius of the 0.4-mm radius insert which enables the reduction of cutting forces and friction between the tool and the workpiece.
- Higher surface roughness values were obtained when the ratio of undeformed chip thickness to cutting edge radius was lower than 1 for the considered workpiece materials due to the negative rake angle. However, the surface roughness values were found to increase as the ratio of undeformed chip thickness to cutting edge radius tend to be higher than 1 for the considered inserts and workpiece materials.
- Side milling with the 48.50-µm cutting edge radius insert resulted in lower surface roughness values due to its lower cutting edge radius when compared with the 68.50 and 98.72-µm cutting edge radii inserts. This is because the 0.4-mm nose radius insert has a smaller cutting edge radius, which makes it sharper and therefore results in lower

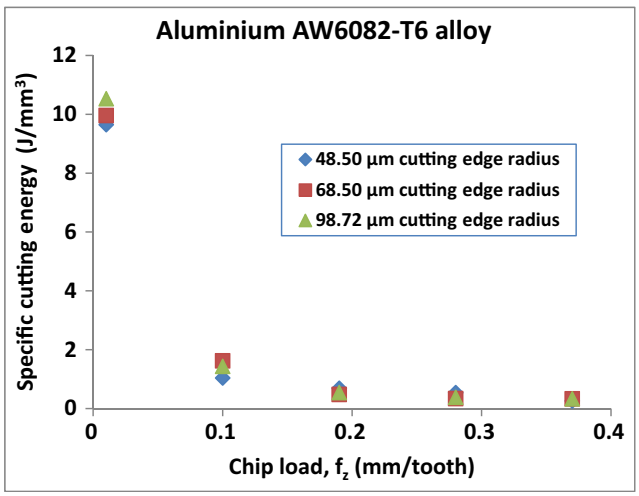

Fig. 6 Variation of specific cutting energy with chip load during side milling of aluminium AW6082-T6 alloy with different cutting edge radii

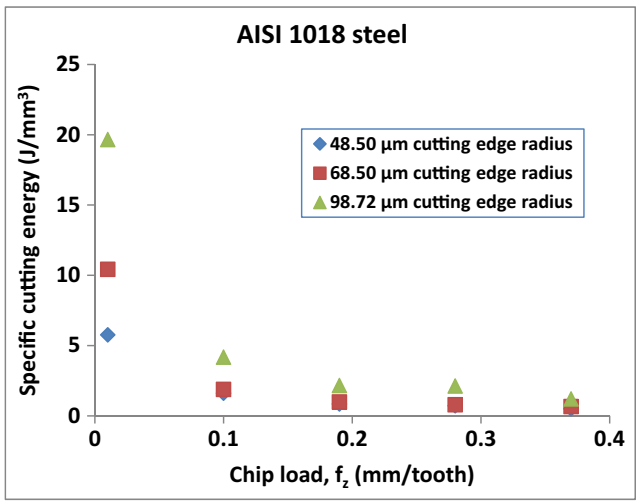

Fig. 7 Variation of specific cutting energy with chip load during side milling of AISI 1018 steel with different cutting edge radii

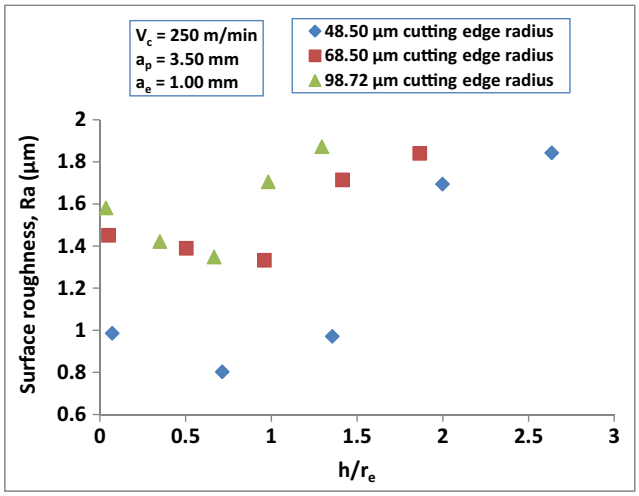

Fig. 8 Variation of surface roughness with ratio of undeformed chip thickness to cutting edge radius during side milling of aluminium AW6082-T6 alloy using different nose radii of inserts

friction between the tool and workpiece, and lower ploughing and rubbing effects. However, machining with large cutting edge radii leaves visible feed marks on the newly machined surface.

- The results also show that energy efficiency in mechanical machining could be improved by machining parts using inserts with smaller cutting edge radius.
- Sustainability index criterion could be improved when evaluated using the ratio of the undeformed chip thickness to the cutting edge radius for all mechanical machining processes. Although undeformed chip thickness, surface roughness, and specific energy trade-offs existed among these variables, sustainability could still be achieved by optimising the desired parameters.
- This work only considered the use of one CNC milling machine. Thus, further studies could be performed using two or more CNC milling machines to further validate the results obtained in this study and generate more machine tool energy data for the life cycle inventory (LCI) and analysis. The LCI data are important to determine the sustainability of any production process in terms of their carbon footprints.

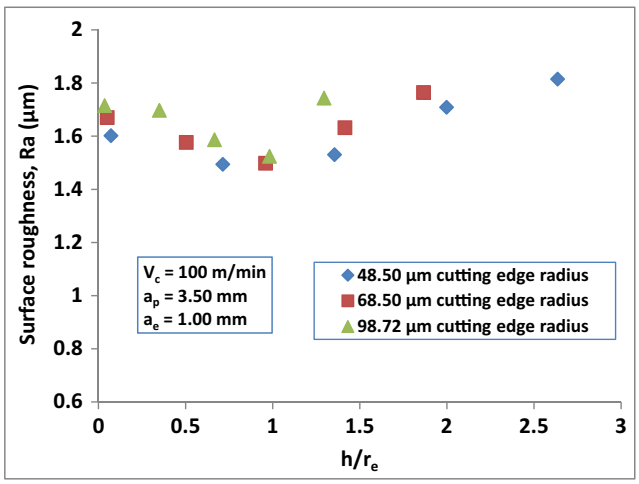

Fig. 9 Variation of surface roughness with ratio of undeformed chip thickness to cutting edge radius during side milling of AISI 1018 steel using different nose radii of insert

References

1. Dahmus JB, Gutowski TG (2004) An environmental analysis of machining, IMECE2004 ASME International Mechanical Engineering Congress and RD&D Expo :1–10
2. Tristo G, Bissacco G, Lebar A, Valentincic J (2015) Real time power consumption monitoring for energy efficiency analysis in micro EDM milling. Int J Adv Manuf Technol. https://doi.org/10.1007/s00170-014-6725-3
3. Gutowski T, Dahmus J, Thiriez A (2006) Electrical energy requirements for manufacturing processes. Proceedings of 13th CIRP International Conference on Life Cycle Eng, Leuven :623
4. Edem IF, Mativenga PT (2017) Modelling of energy demand from computer numerical control (CNC) toolpaths. J Clean Prod 157:310–321
5. Balogun VA, Mativenga PT (2013) Modelling of direct energy requirements in mechanical machining processes. J Clean Prod 41:179–186
6. Edem IF, Mativenga PT (2016) Impact of feed axis on electrical energy demand in mechanical machining processes. J Clean Prod 137:230–240
7. Edem IF, Mativenga PT (2016) Energy demand reduction in milling based on component and toolpath orientations. Procedia Manufacturing 7: 253-261, International Conference on Sustainable Materials Processing and Manufacturing, SMPM 2017, 23–25 January 2017, Kruger National Park
8. ISO 14955-1:2014 Machine tools—environmental evaluation of machine tools—part 1: design methodology for energy-efficient machine tools (2014)
9. Kellens K, Dewulf W, Overcash M, Hauschild Z, Duflou JR (2011) Methodology for systematic analysis and improvement of manufacturing unit process life-cycle inventory (UPLCI)-CO2PE! Initiative (cooperative effort on process emissions in manufacturing). Part 1: methodology description. Int J Life Cycle Assess 17(1):69–78
10. Apostolos F, Alexios P, Georgios P, Panagiotis S, George C (2013) Energy efficiency of manufacturing processes: a critical review. Procedia CIRP 7:628–633
11. Guo Y, Loenders J, Duflou J, Lauwers B (2012) Optimization of energy consumption and surface quality in finish turning. Procedia CIRP 1:512–517
12. Anderberg S, Beno T, Pejryd L (2012) Energy and cost efficiency in CNC machining from a process planning perspective. The 9th Global Conference on Sustainable Manufacturing, Springer
13. Sarwar M, Persson M, Hellbergh H, Haider J (2009) Measurement of specific cutting energy for evaluating the efficiency of bandsawing different workpiece materials. Int J Mach Tools Manuf 49(12–13):958–965
14. Rodrigues AR, Coelho RT (2007) Influence of the tool edge geometry on specific cutting energy at high speed cutting. J Braz Soc Mech Sci Eng 29:279–283
15. Sreejith PS, Krishnamurthy R, Malhotrac SK, Narayanasamy (2000) Evaluation of PCD tool performance during machining of

carbon/phenolic ablative composites. J Mater Proc Technol 104: 53–58
16. Yuan ZJ, Zhou M, Dong S (1996) Effect of diamond tool sharpness on minimum cutting thickness and cutting surface integrity in ultraprecision machining. J Mat Proc Technol 62:327–330
17. Bissacco G, Hansen HN, De Chiffre L (2006) Size effects on surface generation in micro milling of hardened tool steel. CIRP Ann Manuf Technol 55(1):593–596
18. Ducobo F, Filippi E, Riviere-Lorphevre E (2009) Chip formation and minimum chip thickness in micro-milling. Proceedings of the 12th CIRP Conference on Modelling of Machining Operations: 339-346
19. Filiz S, Conley CM, Wasserman MB, Ozdoganlar OB (2007) An experimental investigation of micro-machinability of copper 101 using tungsten carbide micro-endmills. Int J Mach Tools Manuf 47(7–8):1088–1100
20. Balogun VA, Mativenga PT (2014) Impact of un-deformed chip thickness on specific energy in mechanical machining processes. J Clean Prod 69:260–268
21. Balogun VA, Gu H, Mativenga PT (2014) Improving the integrity of specific cutting energy coefficient for energy demand modelling. **Proc Inst Mech Eng B J Eng Manuf**
22. Schluter MS, Hubner HB, Souza AJ (2015) Optimization of cutting parameters for face milling of cast iron by reducing specific cutting energy and machined surface roughness. Appl Mech Mater 727-728:339–344
23. Sealy MP, Liu ZY, Zhang D, Guo YB, Liu ZQ (2015) Energy consumption and modeling in precision hard milling. **J Clean Prod**
24. Liu ZY, Guo YB, Sealy ZQ, Liu ZQ (2016) Energy consumption and process sustainability of hard milling with tool wear progression. J Mat Proc Technol 229:305–312
25. Balogun VA, Edem IF, Adekunle AA, Mativenga PT (2016) Specific energy based evaluation of machining efficiency. J Clean Prod 116:187–197
26. Wang B, Liu Z, Song Q, Wan Y, Shi Z (2016) Proper selection of cutting parameters and cutting tool angle to lower the specific cutting energy during high speed machining of 7050-T7451 aluminum alloy. J Clean Prod 129:292–304
27. Zhou L, Li J, Li F, Xu X, Wang L, Wang G, Kong L (2017) An improved cutting power model of machine tools in milling process. Int J Adv Manuf Technol. https://doi.org/10.1007/s00170-016-9929-x
28. Balogun VA, Edem IF (2017) Optimum swept angle estimation based on the specific cutting energy in milling AISI 1045 steel alloy. Int J Eng Trans A Basics 30(4):591–596
29. Taminiau DA, Dautzenberg JH (1991) Bluntness of the tool and process forces in high-precision cutting. CIRP Ann Manuf Technol 40(1):65–68
30. Waldorf DJ (2006) A simplified model for ploughing forces in turning. J Manuf Proc 8(2):76–82
31. Arif M, Rahman M, San WY (2012) A study on the effect of tool-edge radius on critical machining characteristics in ultra-precision milling of tungsten carbide. Int J Adv Manuf Technol 67(5–8): 1257–1265
32. Zhang T, Liu Z, Shi Z, Xu C (2016) Investigation on size effect of specific cutting energy in mechanical micro-cutting. Int J Adv Manuf Technol 91(5–8):2621–2633
33. Vogler MP, DeVor RE, Kapoor SG (2004) On the modeling and analysis of machining performance in micro-endmilling, part I: surface generation. J Manuf Sci Eng 126(4):685
34. Chou YK, Song H (2004) Tool nose radius effects on finish hard turning. J Mat Proc Technol 148:259–268
35. Jin C-Z, Kang I-S, Park J-H, Jang S-H, Kim J-S (2009) The characteristics of cutting forces in the micro-milling of AISI D2 steel. J Mech Sci Technol 23(10):2823–2829
36. Zhao T, Zhou JM, Bushlya V, Stahl JE (2017) Effect of cutting edge radius on surface roughness and tool wear in hard turning of AISI 52100 steel. Int J Adv Manuf Technol 91(9–12):3611–3618
37. Fulemova J, Janda Z (2014) Influence of the cutting edge radius and the cutting edge preparation on tool life and cutting forces at inserts with wiper geometry. Procedia Engineering 69: 565–573, 24th DAAAM International Symposium on Intelligent Manufacturing and Automation
38. Edem IF, Balogun VA, Mativenga PT (2017) An investigation on the impact of toolpath strategies and machine tool axes configurations on electrical energy demand in mechanical machining. Int J Adv Manuf Technol 92(5–8):2503–2509
39. Ma J, Ge X, Chang SI, Lei S (2014) Assessment of cutting energy consumption and energy efficiency in machining of 4140 steel. Int J Adv Manuf Technol 74(9–12):1701–1708